



Regular article

Influence of hydrogen on incipient plasticity in CoCrFeMnNi high-entropy alloy

Guanghui Yang^{a,1}, Yakai Zhao^{b,1}, Dong-Hyun Lee^c, Jeong-Min Park^a, Moo-Young Seok^c, Jin-Yoo Suh^{d,*}, Upadrasta Ramamurty^e, Jae-il Jang^{a,*}^a Division of Materials Science and Engineering, Hanyang University, Seoul 04763, Republic of Korea^b School of Materials Science and Engineering, Beijing Institute of Technology, Beijing 100081, China^c Max-Planck-Institut für Eisenforschung GmbH, Max-Planck-Straße 1, Düsseldorf 40237, Germany^d High Temperature Energy Materials Research Center, Korea Institute of Science and Technology, Seoul 02792, Republic of Korea^e School of Mechanical and Aerospace Engineering, Nanyang Technological University, Singapore 639798

ARTICLE INFO

Article history:

Received 20 September 2018

Accepted 8 October 2018

Available online 14 October 2018

Keywords:

High-entropy alloy

Hydrogen

Nanoindentation

Vacancy

ABSTRACT

The influence of hydrogen on the onset of plastic deformation in a CoCrFeMnNi high-entropy alloy (HEA) was examined through the analysis of the load at which first pop-in during spherical nanoindentation experiments occurs on hydrogen-charged and subsequently aged specimens. Results reveal that the dissolved hydrogen lowers the plastic flow resistance, indicated by the shear yield strength, τ_y , by modifying defect formation energies. Aging, subsequent to charging, leads to recovery of τ_y , but only partially. The results are discussed in terms of the vacancy-mediated dislocation nucleation, which is supported by the estimated activation volume for deformation.

© 2018 Acta Materialia Inc. Published by Elsevier Ltd. All rights reserved.

High-entropy alloys (HEAs), which contain four or more principal elements of different crystal structures but usually have single (or two) phase microstructure, have recently attracted significant attention due to their unique properties [1–5], such as outstanding cryogenic properties [3,6] and excellent creep [7], corrosion [8], and irradiation [9] resistances. It was reported recently that they are also highly resistant to hydrogen embrittlement (HE) [10,11], which led to a spur in the research activities aimed at understanding the role of hydrogen (H) on the mechanical behavior of HEAs' [12–17]. These studies reveal that HEAs may exhibit limited HE (i.e., small ductility loss upon H charging) in spite of their high H solubility, suggesting the potential of HEA as a future H-tolerant material. Nevertheless, the role of H on the HEAs' fundamental deformation processes (such as dislocation nucleation) and their possible differences from those in conventional alloys are yet to be clarified. Keeping this in view, spherical nanoindentation experiments on a single face-centered cubic (fcc) phase CoCrFeMnNi HEA – one of the most widely investigated HEA to date [3,6,7,11] – are performed in the present study and the loads at which the first pop-ins occur were analyzed. It is well established that the load-displacement (P - h) responses obtained via such experiments often exhibit discrete displacement bursts of displacement (or load drops when tested

under displacement control), which are referred to as “pop-ins” [18–23] and can be utilized for understanding the mechanisms of incipient plasticity [20,21]. For materials with low dislocation densities and step-free surfaces, the first pop-in often corresponds to the dislocation nucleation in the highly stressed region beneath the indenter, which is supported by the observation that the maximum shear stress, τ_{\max} , at pop-in could reach the theoretical shear strength of some materials. In this study, an experimental investigation into the effects of H charging and subsequent aging on the first pop-in was conducted and statistical analyses of the data generated was performed to assess the influence of H on HEA's plastic deformation behavior.

Ingots of equiatomic CoCrFeMnNi HEA were vacuum induction cast by using a mixture of the constituent elemental metals, each with purity higher than 99 wt%. The ingots were hot rolled and then homogenized at 1100 °C for 1 h so as to obtain an alloy with single fcc phase structure [15]. The specimens were initially mechanically polished with sand paper (grit number up to 2000) and then electropolished at 70 V for 60 s at room temperature in a mixture of 90% acetic and 10% perchloric acid. The polished samples were electrochemical charged with H in a 1 N H₂SO₄ solution. Two different sets of charging conditions were utilized. (1) Charging for a fixed time, t_c , of 3 h but with varying current densities, J (= 10, 30, and 100 mA/cm²). (2) Charging with a fixed J of 10 mA/cm² but with varying t_c (3, 12, and 24 h). Additionally, the charged specimens (with J = 10 mA/cm² and t_c = 12 h) were naturally aged at room temperature for different time t_a (24, 48, and 360 h) so as to examine the effect of H desorption on plasticity.

* Corresponding authors.

E-mail addresses: jinyoo@kist.re.kr (J.-Y. Suh), jijang@hanyang.ac.kr (J. Jang).¹ These authors contributed equally to this work.

Nanoindentation tests on uncharged, H-charged, and aged (or discharged) specimens were performed using Nanoindenter-XP (formerly MTS; now KLA-Tencor, Milpitas, CA, USA) with a spherical indenter having tip radius $R = 8.08 \mu\text{m}$ (which was calibrated through Hertzian contact analysis [24,25] of indentations made on fused quartz). More than 50 tests for each condition were conducted at a constant loading rate of $dP/dt = 0.5 \text{ mN s}^{-1}$, where P is indentation load and t is time. All the nanoindentation tests on H-charged samples were performed within 1800 s after H charging to minimize any possible H loss.

Representative P - h curves obtained from spherical nanoindentation experiments on the charged samples are displayed in Fig. 1. Pop-ins can be seen in most of the loading segments. The load corresponding to the first pop-in, P_1 , decreases gradually with an increase in either J or t_c ; no pop-ins were noted for the cases of $J = 100 \text{ mA/cm}^2$ and $t_c = 3 \text{ h}$ (Fig. 1a) and $J = 10 \text{ mA/cm}^2$ and $t_c = 24 \text{ h}$ (Fig. 1b). Since the H content in the alloy can be expected to increase with either J or t_c [26], it is reasonable to conclude that P_1 decreases with increasing H content in the HEA examined.

During spherical indentation, the deformation prior to the first pop-in is purely elastic and hence follows the Hertzian P - h relation [25]: $P = \frac{4}{3} E_r^{0.5} h^{1.5}$ where E_r is the reduced modulus that can be determined by Young's moduli and Poisson's ratios of the specimen and indenter [25]. In Fig. 1, the experimental P - h responses match those predicted using the above relation (dashed lines) until the first pop-in. This confirms that the first pop-in indeed marks the transition from elastic to elasto-plastic deformation. Thus, the value of τ_{max} corresponding to P_1 represents the shear yield strength, τ_y , of the alloy [25]:

$$\tau_y = 0.31p_0 = 0.31 \left(\frac{3}{2} p_m \right) = 0.31 \left(\frac{6E_r^2}{\pi^3 R^2} P_1 \right)^{\frac{1}{3}} \quad (1)$$

Table 1

First pop-in load (P_1) and shear yield stress (τ_y) of uncharged, H-charged, and H-charged-then-aged specimens under different conditions.

		P_1 [mN]	τ_y [GPa]
Uncharged		2.52 ± 0.74	1.99 ± 0.20
H-charged	$10 \text{ mA/cm}^2, 3 \text{ h}$	1.24 ± 0.33	1.56 ± 0.15
	$30 \text{ mA/cm}^2, 3 \text{ h}$	0.70 ± 0.25	1.30 ± 0.16
	$10 \text{ mA/cm}^2, 12 \text{ h}$	0.77 ± 0.18	1.35 ± 0.11
H-charged ($10 \text{ mA/cm}^2, 12 \text{ h}$) then aged	+A24h	0.84 ± 0.27	1.38 ± 0.15
	+A48h	1.33 ± 0.42	1.60 ± 0.17
	+A360h	1.17 ± 0.48	1.53 ± 0.19

where p_0 and p_m are the maximum and mean pressure of the contact, respectively. The calculated τ_y values are listed along with P_1 in Table 1. It is evident that an increase in either J or t_c or both, leads to a reduction in τ_y . This leads to the conclusion that an increase in the H content in the HEA reduces the barrier for either dislocation nucleation and/or multiplication [20,21]. Since well-annealed and electropolished samples are used in the present study and the highly-stressed volume underneath the indenter can be considered small enough for it to be dislocation free [20,27,28], we deduce that dislocation nucleation is the predominant mechanism that results in the first pop-in event. While micro-cracking (of an oxide layer or natural brittleness) can also be responsible for the observed pop-ins [29,30], such a possibility can be ruled out here due to the fact that nanoindentation with a spherical tip at relatively low load was performed, that too on a ductile fcc alloy, making it impossible for the crack formation (even after severe H charging) as there will not be sufficient stored strain energy for such a mechanism to occur. Moreover, if cracking was to be the predominant mechanism for the observed pop-ins, one should expect the opposite

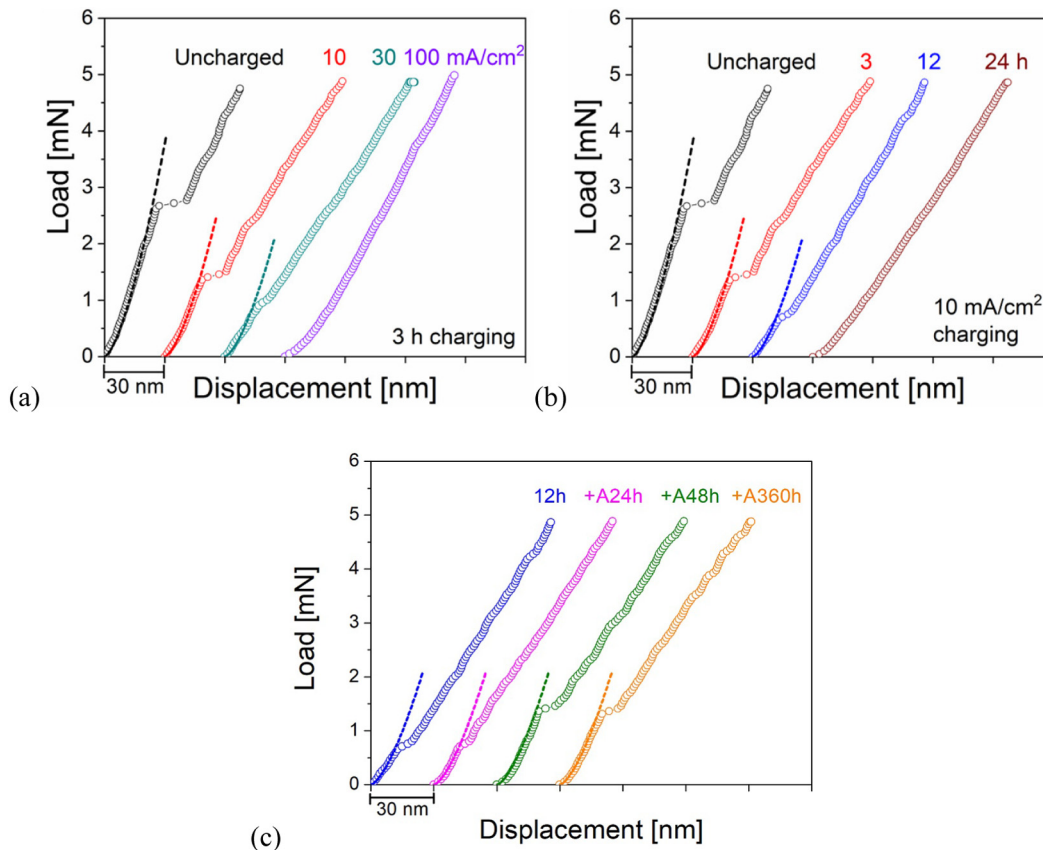


Fig. 1. Representative load-displacement responses (only the loading segments are displayed for clarity) that show the first pop-ins in specimens that are charged with hydrogen (a) for a fixed time of 3 h at different current densities and (b) at a fixed current density of 10 mA/cm^2 for different durations. (c) P - h responses obtained on aged (subsequent to charging for 12 h at 10 mA/cm^2) specimens. The P - h response obtained on pristine (i.e., before charging) sample is also displayed in all the three plots for comparison purposes. Dashed lines in the figures are the Hertzian fitting curves.

trends, i.e., larger pop-ins with higher charging, to those observed experimentally here.

Consequently, the role of H in reducing τ_y can be understood from the thermodynamic framework of so-called “defactants” (originated from “DEfect ACTing AgeNTS” [28,31]) wherein H atoms preferentially segregate to the defect sites (such as dislocations) and, in turn, lower their activation energy (for the formation of dislocation loops in the present case of plasticity initiation). Such a mechanism could lead to the well-known H-enhanced local plasticity (HELP), leading to a reduction in τ_y with increasing J and/or t_c , [28,31]. Pop-ins were not observed in the samples that were subjected to the harshest charging conditions, viz. $J = 100 \text{ mA/cm}^2$ and $t_c = 3 \text{ h}$ (Fig. 1a) and $J = 10 \text{ mA/cm}^2$ and $t_c = 24 \text{ h}$ (Fig. 1b), because the dislocation nucleation becomes much easier and occurs at extremely low loads, which makes it impossible to detect.

It is worth noting here that although H reduces τ_y , a separate study found that the hardness of the same HEA, which was H-charged via the same electrochemical route, increases [10,11]. This divergence between the effect of H on incipient plasticity and hardness is consistent with similar observations made on austenitic stainless steels, which are similar to the present HEA in terms of constituent elements [27,32]. In this context, it is worth noting that while τ_y is controlled by dislocation nucleation, hardness, which typically indicates a material's plastic flow resistance at relatively large strains, is sensitive to dislocation mobility and ability to multiply [33,34]. Thus, the presence of H in an alloy can enhance its strength by promoting slip planarity as well as increase the lattice friction stress for dislocation mobility, both of which hinder dislocation movement [27,32].

In trying to understand the effect of H on dislocation nucleation process, it is important to examine whether it occurs homogeneously or heterogeneously [20,21,35]. In line with the activation energy estimation by Zhu et al. [36], the relatively low τ_y value in the present study (falling within the range of $\sim\mu/46\text{--}\mu/31$, where μ is shear modulus and $\sim 74 \text{ GPa}$ for CoCrFeMnNi [36]) can exclude the homogeneous dislocation nucleation mechanism corresponding to τ_y of theoretical shear yield strength ($\sim\mu/30\text{--}\mu/5$ [35]) and low activation energy. Therefore, a process of heterogeneous dislocation nucleation dominates the incipient plasticity, including several potential atomic-scale mechanisms [37].

In fcc metals and alloys, the binding between H atoms and dislocations is weak, and its trapping energy is slightly smaller than the activation energy required for the bulk diffusion of H atoms [10,38]. Therefore, upon natural aging for sufficiently long durations, H atoms weakly-trapped at dislocation cores can escape from the specimen. Such a scenario should lead to the restoration of τ_y to that in uncharged alloy upon discharging. To examine this possibility, nanoindentation experiments were performed on charged and subsequently aged HEA specimens. Representative $P\text{--}h$ responses of the specimens naturally aged for 24, 48, and 360 h (referred to as +A24h, +A48h, and +A360h, respectively) are displayed in Fig. 1c. They show that P_1 increases with aging, confirming the above hypothesis. However, it is noted from Table 1, where the corresponding τ_y are listed, that the maximum value of τ_y recorded amongst all the aged samples (1.53 GPa in +A360h) is $\sim 23\%$ smaller than τ_y of 1.99 GPa estimated in the uncharged HEA, i.e., only a partial recovery of the strength lost upon H-charging occurs. This observation suggests that the lowering of the dislocation nucleation energy upon H charging may not solely be responsible for the observed reduction in τ_y of HEA upon charging. Hence, additional/complementary mechanistic possibilities need to be invoked.

The interaction between vacancies and H atoms introduced into the lattice via charging supports such mechanism. In H containing metals and alloys, a higher level of equilibrium vacancy concentration exists, which is a result of the attraction between interstitial H and vacancies [39–41]. The trapping of H atoms at defect sites, while simultaneously stabilizing the pre-existing vacancies [31], could also trigger the formation of new vacancies by reducing their formation energy. Estimates of the local H concentration near the surface of an electrochemically charged CoCrFeMnNi HEA made in our prior studies [10,11] show that

it can reach as high as ~ 1143 weight ppm (wppm). Such a high H flux is one of the necessary conditions to induce superabundant vacancy formation [39,42]. Thus, it is possible that a significant enhancement in the concentrations of the vacancies and H-vacancy clusters, both of which can lower the stress required for the onset of plastic deformation, could be the reason behind the incomplete recovery of τ_y even after long-term aging. In a previous study on the same HEA, we observed that the intensity of the high-temperature peak of thermal desorption spectrum remains invariant with increasing aging time whereas the low-temperature peak continuously decreases [10]. This suggests that H atoms easily escape from the weak trapping sites such as dislocations and grain boundaries upon aging while remain unaffected in strong trapping sites which are likely to be vacancies.

Further support for the above proposed vacancy-related mechanism was obtained via the cumulative probability analysis, F , of τ_y data to obtain the activation volume for deformation that causes the pop-ins suggested by Schuh et al. [37,43], as following. Variations in F of τ_y are displayed in Fig. 2a and b. They can be described as a function of the shear stress beneath the indenter, τ :

$$\ln[-\ln(1-F)] = \left\{ -\frac{\Delta G^*}{kT} + \ln\left[\frac{kT\dot{\gamma}_0}{V^*(d\tau/dt)}\right] \right\} + \frac{\tau}{kT}V^* \quad (2)$$

where k is the Boltzmann constant, T is the temperature, $\dot{\gamma}_0$ is the attempt frequency (that is the frequency of the fundamental mode vibration along the reaction pathway), and ΔG^* and V^* are the Helmholtz activation energy and volume of the yielding event, respectively. Note that $d\tau/dt$ is a constant for the present set of nanoindentation tests as they were conducted with a fixed loading rate of dP/dt . Thus, V^* is

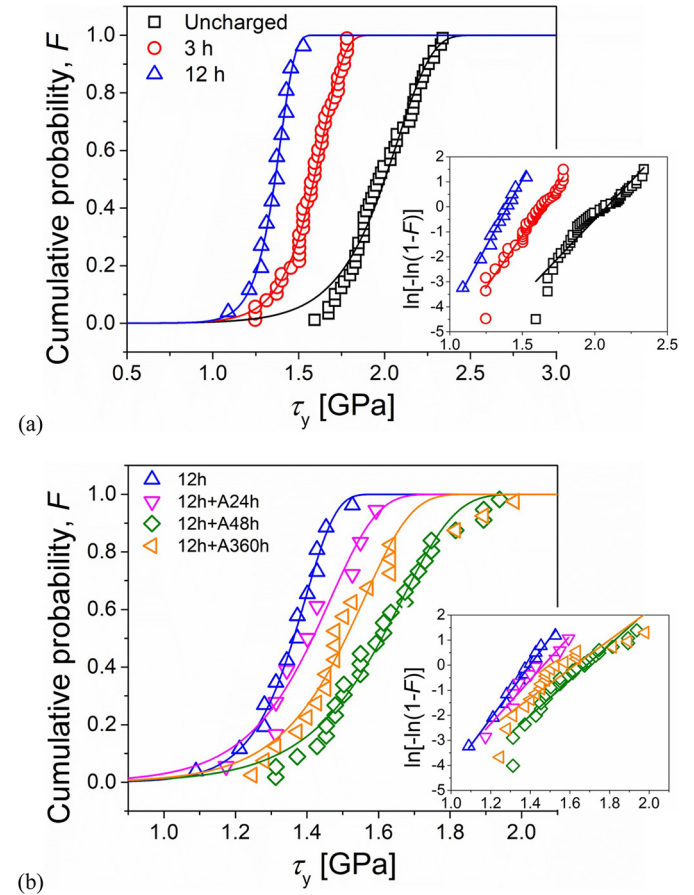


Fig. 2. Cumulative probability distribution of τ_y . Insets showing linear fits of the $\ln[-\ln(1-F)]$ vs. τ_y plot employed to estimate the activation volume; (a) uncharged and H-charged specimens and (b) 12-h-charged and subsequently aged specimens.

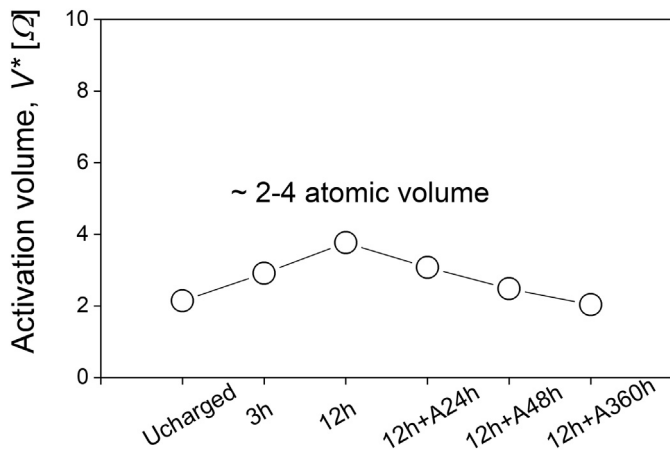


Fig. 3. The estimated activation volume for the onset of plasticity.

estimated from the slope of $\ln[-\ln(1 - F)]$ vs. τ_y plots [44] and is expressed as a function of the atomic volume, Ω , through the relation $\Omega = 0.25a^3$ [36] where a is the lattice parameter ($= 3.594 \text{ \AA}$ [15] for the current HEA with fcc crystal structure). Variation in V^* with H charging and subsequent aging sequences displayed in Fig. 3 shows that it is

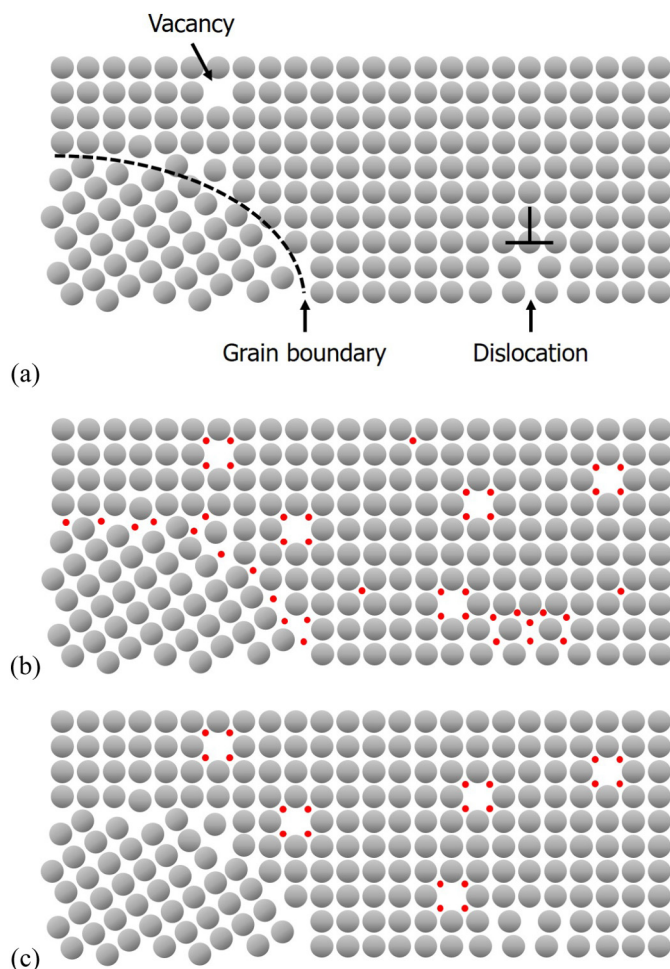


Fig. 4. A two-dimensional schematic illustration of the microstructure states at (a) uncharged, (b) charged, and (c) discharged (for sufficiently long duration), where grey solid circles represent metallic atoms in HEAs, red solid circles represent H atoms. For the sake of simplicity, different atoms in HEA are not distinguished and only edge dislocation is presented.

in the range of $\sim 2\text{--}4\Omega$, which is relatively insignificant as far as V^* are typically noted for. The range is in a good agreement with Zhu et al.'s [36] study where a V^* of the order of 3Ω was obtained. For comparison, V^* for fcc Pt and Ni are $\sim 0.5\Omega$ and $\sim 1\Omega$, respectively, suggesting the migration of individual point-like defects [35,37,45]. Therefore, a large V^* in the examined HEA indicates that a vacancy or vacancy cluster related process can be the predominant rate-limiting mechanism for the onset of plasticity. On this basis, we suggest that the fundamental mechanism governing the onset of plasticity is the vacancy-mediated heterogeneous dislocation nucleation involving cooperative motion of several atoms [36,45]. Further, it is useful for rationalizing the observed variations in τ_y of the HEA upon H charging and subsequent aging as following (schematically illustrated in Fig. 4). In the uncharged state (Fig. 4a), various crystalline defects (including dislocations, grain boundaries, and vacancies) exist and play the usual role in the plastic deformation. Upon charging with H (Fig. 4b), H atoms occupy interstitial sites and interact with aforementioned defects, and at the same time, superabundant vacancies are introduced into the lattice of the HEA, such that the vacancy-mediated heterogeneous dislocation nucleation in the CoCrFeMnNi HEA is promoted due to the H's role in defect activation, leading to the observed reduction in τ_y . Aging of the charged alloy at room temperature (Fig. 4c) leads to the desorption of the H atoms located at interstitial sites, dislocations, and grain boundaries, but the H-induced vacancies and the H atoms strongly trapped there remain, causing only a partial recovery of τ_y .

In summary, the influence of H charging on the incipient yielding behavior of the CoCrFeMnNi HEA was investigated by spherical nanoindentation experiments and statistical analysis of the first pop-in load data. Results and analysis show that the onset of plasticity underneath the indenter is governed by vacancy-mediated heterogeneous dislocation nucleation in the well annealed HEA. Charging of it with H markedly reduces the shear yield strength due to the modification of the formation energy of dislocation loops and vacancies. Aging, subsequent to charging, does not lead to the full recovery of the strength; such partial recovery is attributed to the remnant H-vacancy clusters.

The work at Hanyang University was supported by the National Research Foundation of Korea (NRF) grants funded by the Ministry of Science and ICT (No. 2015R1A5A1037627 and No. 2017R1A2B4012255). YZ would like to thank the support from the project funded by China Postdoctoral Science Foundation (No. 2017M620638). JYS would like to thank the support from Korea Institute of Science and Technology (2W28060).

References

- [1] B. Cantor, I.T.H. Chang, P. Knight, A. Vincent, *Mater. Sci. Eng. A* 375–377 (2004) 213–218.
- [2] J.-W. Yeh, S.-K. Chen, S.-J. Lin, J.-Y. Gan, T.-S. Chin, T.-T. Shun, C.-H. Tsau, S.-Y. Chang, *Adv. Eng. Mater.* 6 (2004) 299–303.
- [3] B. Gludovatz, A. Hohenwarter, D. Catoor, E.H. Chang, E.P. George, R.O. Ritchie, *Science* 345 (2014) 1153–1158.
- [4] Z. Li, K.G. Pradeep, Y. Deng, D. Raabe, C.C. Tasan, *Nature* 534 (2016) 227–230.
- [5] D.B. Miracle, O.N. Senkov, *Acta Mater.* 122 (2017) 448–511.
- [6] F. Otto, A. Dlouhý, Ch. Somsen, H. Bei, G. Eggeler, E.P. George, *Acta Mater.* 61 (2013) 5743–5755.
- [7] D.-H. Lee, M.-Y. Seok, Y. Zhao, I.-C. Choi, J. He, Z. Lu, J.-Y. Suh, U. Ramamurty, M. Kawasaki, T.G. Langdon, J.-i. Jang, *Acta Mater.* 109 (2016) 314–322.
- [8] Y. Shi, B. Yang, P.K. Liaw, *Metals* 7 (2017) 43.
- [9] K. Jin, H. Bei, *Front. Mater.* 5 (2018) 26.
- [10] Y. Zhao, D.-H. Lee, J.-A. Lee, W.-J. Kim, H.N. Han, U. Ramamurty, J.-Y. Suh, J.-i. Jang, *Int. J. Hydrog. Energy* 42 (2017) 12015–12021.
- [11] Y. Zhao, D.-H. Lee, M.-Y. Seok, J.-A. Lee, M.P. Phaniraj, J.-Y. Suh, H.-Y. Ha, J.-Y. Kim, U. Ramamurty, J.-i. Jang, *Scr. Mater.* 135 (2017) 54–58.
- [12] H. Luo, Z. Li, D. Raabe, *Sci. Rep.* 7 (2017) 9892.
- [13] H. Luo, Z. Li, W. Lu, D. Ponge, D. Raabe, *Corros. Sci.* 136 (2018) 403–408.
- [14] K.E. Nygren, K.M. Bertsch, S. Wang, H. Bei, A. Nagao, I.M. Robertson, *Curr. Opin. Solid State Mater. Sci.* 22 (2018) 1–7.
- [15] Y. Zhao, D.-H. Lee, W.-J. Kim, M.-Y. Seok, J.-Y. Kim, H.N. Han, J.-Y. Suh, U. Ramamurty, J.-i. Jang, *Mater. Sci. Eng. A* 718 (2018) 43–47.
- [16] K. Ichii, M. Koyama, C.C. Tasan, K. Tsuzaki, *Scr. Mater.* 150 (2018) 74–77.
- [17] Y.J. Kwon, J.W. Won, S.H. Park, J.H. Lee, K.R. Lim, Y.S. Na, C.S. Lee, *Mater. Sci. Eng. A* 732 (2018) 105–111.

- [18] T.F. Page, W.C. Oliver, C.J. McHargue, *J. Mater. Res.* 7 (1992) 450–473.
- [19] W.A. Soer, K.E. Aifantis, J.Th.M. De Hosson, *Acta Mater.* 53 (2005) 4665–4676.
- [20] H. Bei, Y.F. Gao, S. Shim, E.P. George, G.M. Pharr, *Phys. Rev. B* 77 (2008), 060103.
- [21] J.-i. Jang, H. Bei, P.F. Becher, G.M. Pharr, *J. Am. Ceram. Soc.* 95 (2012) 2113–2115.
- [22] Y. Zhao, I.-C. Choi, M.-Y. Seok, M.-H. Kim, D.-H. Kim, U. Ramamurty, J.-Y. Suh, J.-i. Jang, *Acta Mater.* 78 (2014) 213–221.
- [23] Y. Gao, H. Bei, *Prog. Mater. Sci.* 82 (2016) 118–150.
- [24] K.L. Johnson, *Contact Mechanics*, Cambridge University Press, Cambridge, 1985.
- [25] W.C. Oliver, G.M. Pharr, *J. Mater. Res.* 19 (2004) 3–20.
- [26] Y. Yao, X. Pang, K. Gao, *Int. J. Hydrog. Energy* 36 (2011) 5729–5738.
- [27] K.A. Nibur, D.F. Bahr, B.P. Somerday, *Acta Mater.* 54 (2006) 2677–2684.
- [28] A. Barnoush, H. Vehoff, *Acta Mater.* 58 (2010) 5274–5285.
- [29] D.E. Kramer, K.B. Yoder, W.W. Gerberich, *Phil. Mag. A* 81 (2001) 2033–2058.
- [30] J.S. Field, M.V. Swain, R.D. Dukino, *J. Mater. Res.* 18 (2003) 1412–1419.
- [31] R. Kirchheim, *Scr. Mater.* 62 (2010) 67–70.
- [32] A. Barnoush, M. Asgari, R. Johnson, *Scr. Mater.* 66 (2012) 414–417.
- [33] T. Ohmura, K. Tsuzaki, *J. Mater. Sci.* 42 (2007) 1728–1732.
- [34] Y. Zhao, I.-C. Choi, Y.-J. Kim, J.-i. Jang, *J. Alloys Compd.* 582 (2014) 141–145.
- [35] L. Wang, H. Bei, T.L. Li, Y.F. Gao, E.P. George, T.G. Nieh, *Scr. Mater.* 65 (2011) 179–182.
- [36] C. Zhu, Z.P. Lu, T.G. Nieh, *Acta Mater.* 61 (2013) 2993–3001.
- [37] C.A. Schuh, J.K. Mason, A.C. Lund, *Nat. Mater.* 4 (2005) 617–621.
- [38] S.-M. Lee, J.-Y. Lee, *Metall. Trans. A* 17 (1986) 181–187.
- [39] Y. Fukai, *J. Alloys Compd.* 356–357 (2003) 263–269.
- [40] M. Nagumo, *Mater. Sci. Technol.* 20 (2004) 940–950.
- [41] S. Lawrence, Y. Yagodzinsky, H. Hännien, E. Korhonen, F. Tuomisto, Z.D. Harris, B.P. Somerday, *Acta Mater.* 128 (2017) 218–226.
- [42] H. Osono, T. Kino, Y. Kurokawa, Y. Fukai, *J. Alloys Compd.* 231 (1995) 41–45.
- [43] C.A. Schuh, A.C. Lund, *J. Mater. Res.* 19 (2004) 2152–2158.
- [44] I.-C. Choi, D.-H. Lee, B. Ahn, K. Durst, M. Kawasaki, T.G. Langdon, J.-i. Jang, *Scr. Mater.* 94 (2015) 44–47.
- [45] Y.X. Ye, Z.P. Lu, T.G. Nieh, *Scr. Mater.* 130 (2017) 64–68.